Proceedings in Manufacturing Systems, Volume 19, Issue 1, 2024, 3-16 ISSN 2067-9238

MODELING AND PARAMETERIZATION OF FLEXIBLE CONSIGNMENTS USING MULTI FLEXIBLE BODY DYNAMICS

Gabriel LEITNER[1,*], Dominik STADLTHANNER[2], Alexander ORTNER-PICHLER[3], Christian LANDSCHÜTZER[4]

[1)] Dipl.-Ing., Research Assistant, Graz University of Technology, Institute of Logistics Engineering, Graz, Austria
[2)] Dipl.-Ing., Research Assistant, Graz University of Technology, Institute of Logistics Engineering, Graz, Austria
[3)] Dipl.-Ing. Dr.techn., Project-Senior Scientist, Graz University of Technology, Institute of Logistics Engineering, Graz, Austria
[4)] Assoc. Prof. Dipl.-Ing. Dr.techn. Prof.h.c., Deputy Head / Prof. for Materials Handling, Graz University of Technology, Institute of Logistics Engineering, Graz, Austria

Abstract: *The courier, express, and parcel (CEP) industry is undergoing a shift in the type of shipments towards dimensionally unstable consignments, presenting novel challenges for sorting and conveying systems operators. Previous simulation approaches are limited in their ability to model all relevant operating principles. To address this gap, this paper presents a structured approach to develop a simulation model that comprehensively represents the motion behavior of dimensionally unstable consignments. The proposed approach comprises four main steps, with this paper focusing on steps 3 and 4. In step 3, four different types of small consignments with flexible packaging are modeled using Multi Flexible Body Dynamics (MFBD), which involves a bottom-up approach to modeling packaging and contents into consignment models. Step 4 involves parameterization, where real-world tests are leveraged to determine target values, alongside the utilization of Design of Experiments (DoE) to explore the effects of model parameters in corresponding simulations. Surrogate models are subsequently employed for parameter optimization to determine parameter values. Finally, to evaluate the practical feasibility of these models, the bulk behavior of multiple consignments on a conveyor belt is simulated. The resulting simulation is capable of modeling the shape instability of consignments with a high level of detail and reasonable computing times. This work makes a significant contribution to the advancement of the simulation of the motion behavior of dimensionally unstable consignments in the sorting process and thus supports the development of innovative sorting and conveying technologies.*

Key words: *CEP, Polybag, MFBD, FMBD, Multi Flexible Body Dynamics, DoE, Parameterization.*

1. INTRODUCTION

In recent years, the courier, express, and parcel (CEP) industry has experienced a tremendous increase in the volume of shipments processed (see Fig. 1). In 2021 alone, the parcel volume increased by 11.2%. The Bundesverband Paket und Expresslogistik e. V. (BIEK) predicts that in Germany, the volume of shipments will rise to around 4.8 billion per year by 2027 [1].

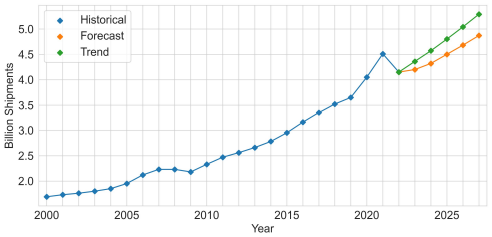

Fig. 1. The forecasted development of the courier, express, and parcel shipment volume until 2027 [1].

* Corresponding author: Graz University of Technology, Inffeldgasse 25e, 8010 Graz, Austria,
Tel.: +43 316 873 7830;
E-mail address: *gabriel.leitner@tugraz.at* (G. Leitner)

Furthermore, the CEP industry has experienced a shift away from traditional cardboard boxes towards small consignments, usually featuring flexible packaging, in recent years. This shift has mainly been driven by the substantial increase in e-commerce and the growing importance of China in online retail. Schadler et al. [2] propose to classify such small consignments, which cannot be categorized as either parcels or letters, under the term "polybags" (see Fig. 2).

Conventional sorting and conveying technologies often do not ensure error-free handling of such flexible consignments. In such cases, manual intervention in the sorting process is required, leading to a significant reduction in throughput and higher processing costs for small consignments. Developing new sorting solutions for these types of shipments is challenging because their

Fig. 2. Polybags [2].

behavior during movement is not yet sufficiently understood. While research on form-stable cardboard packages is already extensive [3–7] research on flexible consignments is still in its infancy. The characterization of polybags has already been carried out by Schadler et al. [2]. A preliminary approach to investigating flexible consignments through simulation has been implemented by Roth [9] using redirection tests, modeling consignments through a "lumped-mass model"[1].

Additionally, a concept for an innovative sorting system specifically for polybags has been presented by Schedler and Landschützer [11], taking into account flow effects through CFD simulations. However, the mentioned simulation approaches are limited in their ability to represent all relevant principles for processing polybags. Moreover, due to their long computational times, they are currently not economically feasible.

Research at the Institute of Logistics Engineering (Graz University of Technology) addresses this gap. Leitner et al. [12] introduced a methodology consisting of four main steps, aimed at systematically studying consignments to gain insight into their movement behavior through a novel simulation approach. Previous research by Schadler et al. [8] laid the groundwork for Step 1 by identifying specific properties of such consignments. Building upon this, Leitner et al. [12] detailed modeling possibilities in Step 2. This paper focuses on enhancing Steps 3 and 4 of the methodology: the modeling if real consignments and the parameterization of the developed models.

The objective of this endeavor is to model the movement behavior of individual flexible consignments using multi flexible body dynamics (MFBD), which combines multi-body dynamics (MBD) and the finite element analysis (FEA). Although MFBD has been employed in the field of mechanics for a considerable period of time, its potential for application in the domain of logistics has not yet been fully realized. The primary focus lies in assessing the feasibility of this approach and establishing a systematic methodology.

The challenge lies in realistically integrating relevant effects into the model without disproportionately increasing the modeling effort and computing time. Therefore, finding a balance between obtaining the desired information and not overburdening resources is crucial. The ultimate goal is to contribute to the development of new sorting and conveying technologies.

2. MULTI FLEXIBLE BODY DYNAMICS

Multi flexible body dynamics is a fusion of the research areas of multi-body dynamics and the finite element analysis. An MFBD system can be considered as a model that includes different rigid and flexible bodies as well as joint and force elements between these bodies (see Fig. 3). It takes into account the fundamental properties of dynamics, such as non-linearity, large deformations, large displacements and large rotations [13].

[1] A lumped mass model uses the principles of multi-body dynamics to model elastic structures. Although it uses a simplified discretization, it can already effectively represent the dynamics of elastic systems with strong nonlinear deformations [5].

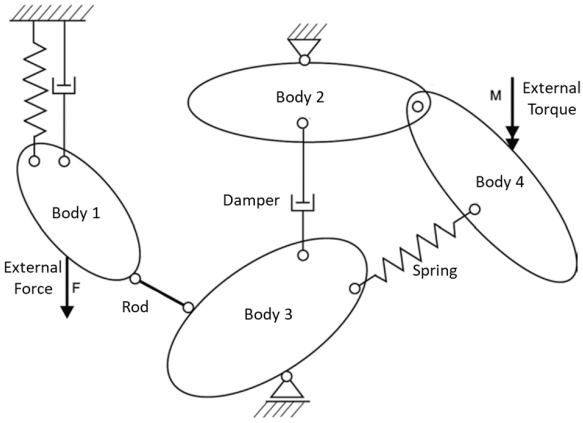

Fig. 3. Model of a general multi-body system [14].

Different approaches have been explored that attempt to couple the two areas [15]. The approach in which the multi-body system capabilities are implemented in existing finite element algorithms proved to be an efficient solution. An incremental finite element formulation based on the co-rotation method is used [13].

This incremental finite element formulation divides the motion of the element into rigid and purely deformable components. By using a local, element-related coordinate system that continuously moves and rotates with the element, any contribution to the rigid body motion is eliminated from the global displacement field to determine the pure deformation. The schematic diagram for the incremental formulation with co-rotation method is shown in Fig. 4 [16].

In order to allow conventional joint and force elements of multi-body dynamics to act on the FEA bodies, the nodes of the FEA bodies are superimposed with virtual, massless rigid bodies and linked to these nodes by means of kinematic admissibility conditions (see Fig. 5).

This approach has the advantage of using only one solver and being able to compute large deformations and non-linearities. Using an MBD-FEA co-simulation would result in a loss of efficiency due to communication between the calculation programs and their solvers.

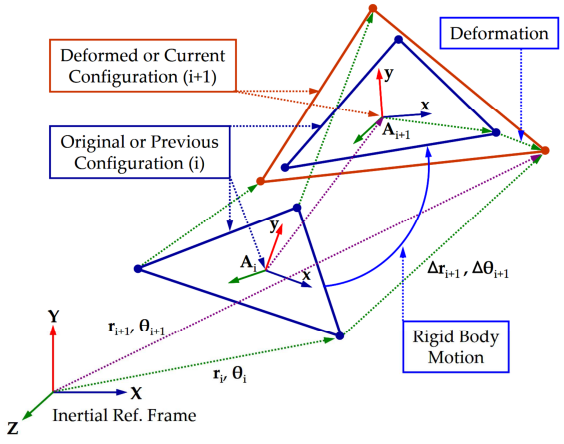

Fig. 4. Schematic diagram of the incremental formulation with the co-rotation method [16].

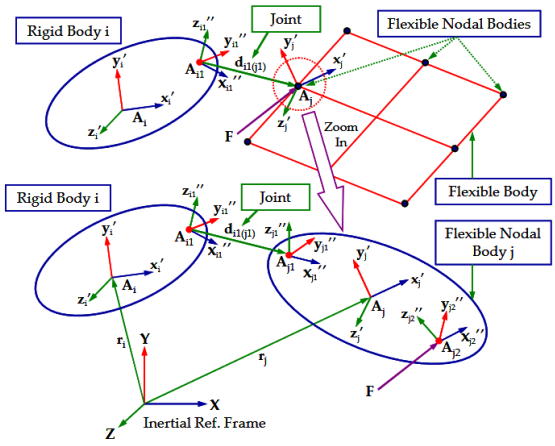

Fig. 5. The coordinate systems for two adjacent rigid and flexible bodies [17].

When using modally reduced solids, only small linear deformations can be accurately realized in a MBD simulation, where the FEA is only used as a pre-processor to calculate the eigenmodes of the elastic bodies [15].

2.1. Contact forces and friction

In addition to joints, bodies can interact through force-controlled free relationships, such as contact conditions with friction. Friction and contact behavior are discrete events that occur when certain conditions are met. The numerical treatment of these variants is challenging and resource-intensive, especially in the case of static friction where there are several possible state values for an input variable [7].

When two bodies come into contact, they undergo elastic or elastic-plastic deformations, resulting in contact forces. The contact plane is defined by the normal vector, and the resulting contact force can be divided into a normal force and a friction force. The normal force is determined by the penetration depth s and its time derivative $\dot{s}$ and is based on a unilaterally acting linear spring-damper element. Coulomb's friction law determines the friction force, which is proportional to both the normal force and the sliding velocity. To avoid numerical problems, a continuous function is often utilized, but it cannot differentiate between static and dynamic friction (see Fig. 6).

Commercial multi-body dynamics programs often extend this simple method of contact calculation to more realistic contact models. The RecurDyn simulation software will now be used as an example to illustrate the calculation of normal force and friction force.

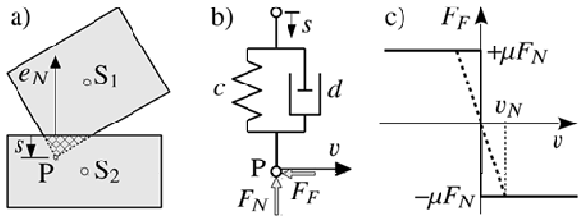

Fig. 6. Simple contact element with: *a* – virtual penetration *s*, *b* – normal force F_N, and *c* – frictional force F_F [10].

The normal force is divided into the spring force and the damping force:

$$F_N = F_{NC} + F_{ND}. \tag{1}$$

The spring force is composed as follows:

$$F_{NC} = c \cdot s^{m_s}. \tag{2}$$

Here c is the stiffness coefficient, s the penetration depth and m_s the stiffness exponent. The stiffness exponent can be used to model non-linear springs.

The user has two options for the damping force. The first option is to use a STEP function:

$$F_{ND} = STEP(s, 0, 0, s_{max}, d) \cdot \dot{s}. \tag{3}$$

STEP functions[2] are used due to their good differentiability and the introduction of a smooth transition instead of an abrupt jump for improved numerical tractability [7]. In this case, the damping coefficient is gradually regulated from zero to the maximum penetration depth.

From this point $F_{ND} = d \cdot \dot{s}$, applies as long as s does not fall below s_{max} (see Fig. 7).

The second option is called the indentation method and is defined as follows:

$$F_{ND} = d \frac{\dot{s}}{|\dot{s}|} |\dot{s}|^{m_d} s^{m_i}. \tag{4}$$

Here d is the damping coefficient, $\dot{s}$ is the time derivative of the indentation depth, m_d is the damping exponent and m_i is the indentation exponent.

However, neither of these options can guarantee that the resulting normal force will not become negative, which would result in unrealistic behavior. Therefore, a minimum normal force is defined:

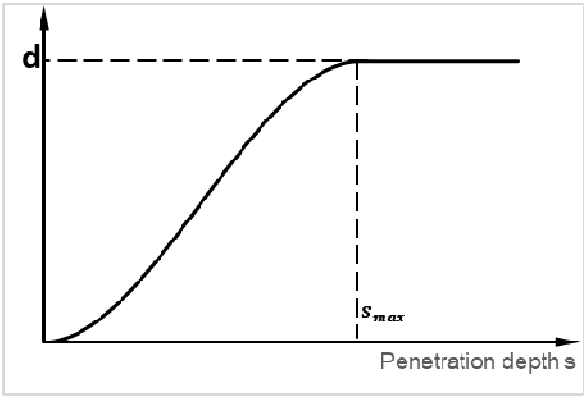

Fig. 7. STEP function for determining the damping in the contact.

[2] The step function approximated by a fourth-order polynomial is a continuously differentiable function, while the step function approximated by a fifth-order polynomial is a two-fold continuously differentiable function.

$$F_{N\_min} = R_{df} \cdot F_{NC}. \quad (5)$$

Here, the rebound damping factor R_{df}, which ranges from zero to one, reduces the spring force F_{NC}.

The equation (6) ensures that the larger of the two force formulations from (1) and (5) is ultimately used. In this way, a negative normal force is avoided and improved separation of the contacts is ensured.

$$F_N = Max\left[F_{NC} + F_{ND}, F_{N\_min}\right] \quad (6)$$

Figure 6 shows an exemplary force curve of a contact process for better illustration. The indentation method is used for the damping force. In this case, F_N (represented by a solid line) is $F_N = F_{NC} + F_{ND}$ during the penetration phase and changes to $F_N = F_{N\_min}$ in the separation phase when $F_{NC} + F_{ND} < F_{N\_min}$, according to formula (6).

The friction force in RecurDyn is calculated according to the following formula:

$$F_F = |\mu(v)| \cdot F_N \cdot \frac{v}{|v|}. \quad (7)$$

Here, the coefficient of friction is not a constant, but depends on the relative velocity. This relationship is shown in

Fig. 9. Here μ_s, μ_d, v_s and v_d stand for the static coefficient of friction, the dynamic coefficient of friction, the static threshold speed and the dynamic threshold speed. Step5 functions are used for a numerically simple calculation of the coefficient of friction:

$$\mu = STEP5(v, -v_s, \mu_s, v_s, -\mu_s) \text{ for } |v| \leq v_s, \quad (8)$$

$$\mu = STEP5(|v|, v_s, \mu_s, v_d, \mu_d) \text{ for } v_s < |v| \leq v_d, \quad (9)$$

$$\mu = \mu_d \text{ for } |v| > v_d. \quad (10)$$

It should be noted that no real adhesion can be realized here either. For a more realistic sticking effect, the user can also select the implemented Sliding & Stiction Type. With this option, the slip in the stationary state is reduced to almost zero. Further information on this can be found in the manual for RecurDyn [15].

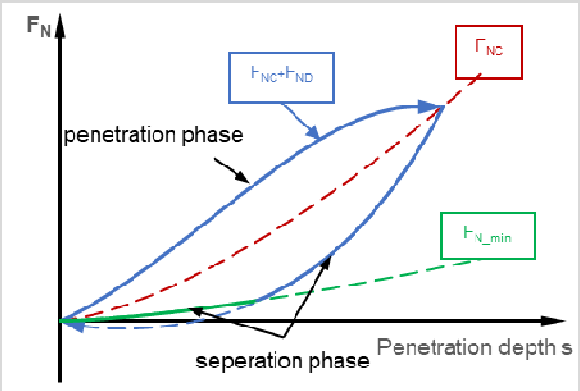

Fig. 8. The hysteresis loop of a contact process. Based on [18].

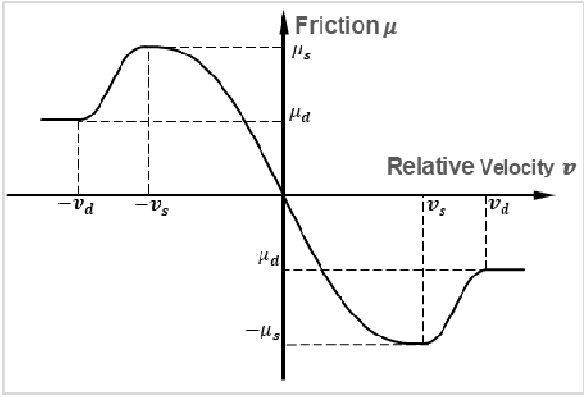

Fig. 9. Relationship between coefficient of friction and relative velocity.

3. METHOD

Efficient transportation of flexible consignments is crucial in various industries and requires a deep understanding of their behavior during transit. This chapter presents a methodology, which was originally outlined in less detail by Leitner et al. [12], for systematically studying consignments to gain insight into their movement behavior. The methodology consists of four main steps, as shown in Fig. 10.

Previous research by Schadler et al. [8] laid the groundwork for Step 1 by identifying specific properties of such consignments. For Step 2, Leitner et al. [XX] described the modeling possibilities. Building upon this foundation, this paper focuses on enhancing Steps 3 and 4 of the methodology and applying them to model real-world consignments and parameterize the developed models.

Step 3: Modeling of real consignments using MFBD

In this step, real consignments are modeled using the MFBD approach. After selecting concrete consignments, the abstract modeling approach from step 2 is applied to these specimens. This involves a bottom-up modeling approach, which includes submodels for packaging and content that are combined into the consignment model. This results in a realistic representation of the real consignments in the simulation environment.

Step 4: Parameterization of the consignment models

This step involves selecting a set of *n* simple yet informative experiments to minimize real-world effort and simulation time for investigating crucial model parameters.

In real-world tests, target values are measured, while corresponding simulations are used to determine the effects of model parameters using Design of Experiments (DoE). If there are more than two parameters of interest, a screening is conducted to determine the significant parameters for the corresponding experiments. After discarding non-significant parameters, a detailed examination of the remaining parameters is conducted, followed by the use of Gaussian Process Regression to construct surrogate models. These models serve as efficient approximations, allowing for the optimization

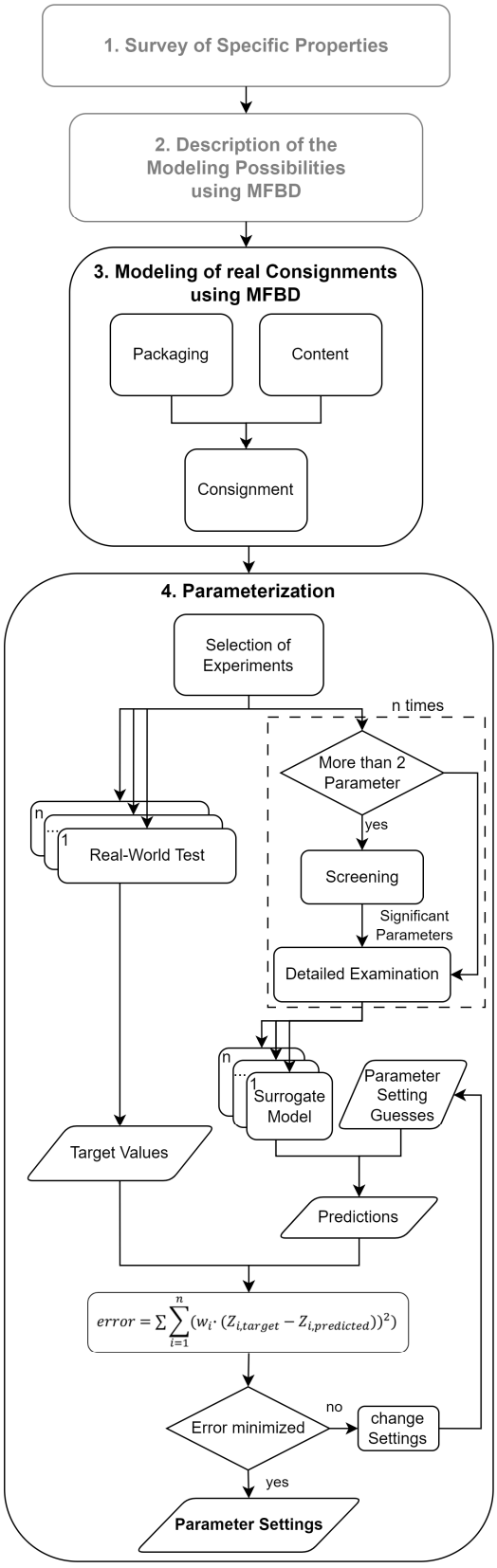

Fig. 10. Flowchart outlining the methodology used in this study. The steps "real-world tests", "surrogate model" and the area marked by the dashed rectangle are repeated n times, where n is the number of target values and depends on the specific problem.

of parameter values. The objective of this task is to minimize the error (see Eq. (11)) between predictions generated by surrogate models and the target values obtained from real-world experiments.

The error function, defined as the sum of the squared weighted differences between predicted responses and target values is expressed mathematically as:

$$error = \sum \sum_{i=1}^{n} (w_i \cdot (Z_{i,target} - Z_{i,predicted}))^2) \quad .(11)$$

Where n is the number of target values, w_i denotes the weight assigned for each model, $Z_{i,predicted}$ represents the predicted response generated by the surrogate model for the i^{th} model and $Z_{i,target}$ denotes the corresponding target value obtained from real-world experiments.

To optimize the parameter values, the minimize function from the Python scikit-learn [19] module is employed, which utilizes the Nelder-Mead [20] optimization method. This function aims to minimize the defined objective function by iteratively adjusting the input parameter values, leading ultimately to the resulting parameter settings.

Selection of a specific consignment

The appropriate selection of a specific consignment is central. It should serve as a representative example for a large number of consignments. Packaging material, shape, dimensions, and content are, among others, important parameters that need to be defined. A major challenge in selecting appropriate specimens to study the physical behavior of these types of consignments is the nearly infinite number of ways in which these characteristics can be combined.

Stadlthanner et al. [21] proposed a clustering approach to address this problem. In their study, a total of 657 consignments were randomly selected from an Austrian distribution center and categorized according to several parameters. In addition to measuring the dimensions and weighing the consignments, the study also considered the packaging material, shape, filling level, flexibility, mobility of the contents, and whether the contents were single or multi-part.

The filling level was categorized using numbers from 1 to 4, where 1 represents less than 25%, 2 represents 25% to 50%, 3 represents 50% to 75%, and 4 represents more than 75%. Flexibility was categorized through overhang tests[3] where the overhang angles were measured. A scale ranging from 1 to 3 was utilized to indicate the degree of overhang. A rating of 1 corresponds to an overhang of less than 5 °, while a rating of 2 corresponds to an overhang of 5 ° to 45 °, and a rating of 3 corresponds to an overhang of more than 45 °.

The collected data, comprising both numerical and categorical features, was homogenized using Gower's

[3] The consignments were put on the edge of a table, with about 1/3 of the length of each consignment being fixed to the top of the table while the other 2/3 were allowed to hang freely over the edge. The resulting angle was then measured to determine the level of flexibility.

distance [22] and clustered using the HDBSCAN algorithm [23]. There was a total of six clusters, each representing a collection of similar consignments from the original dataset. The centroids of these clusters are provided in Table 1.

Due to time and budget constraints, only four of these six centroids were selected as templates for the investigations conducted in the present study (see Fig. 11). To achieve a selection with maximum diversity, cluster centroids two and five were discarded, as they are most similar to the remaining clusters based on Gower's distance. Physical specimens of the four selected cluster centroids were then produced. First, suitable packaging was purchased, with the packaging material corresponding to the respective cluster centroids and the dimensions as close as possible to the target specifications. For cluster centroids 1, 4 and 6, appropriately sized cardboard boxes with respect to the target filling levels were used as content. These cardboard boxes were then filled with two granulates of different densities (perlite and expanded clay aggregate), with the mass ratio chosen to match the target masses of each cluster centroid. For cluster centroid 3, which features a flexible content, the granulates where instead put in a plastic bag which was then placed inside the packaging. Clusters 3, 4 and 6 have non-movable contents. In the case of cluster 4, adhesive strips were used to secure the contents to the packaging, while in the other two cases this was not necessary due to the tight-fitting packaging. The dimensions of the resulting four consignments and the corresponding contents are summarized in Table 2.

Due to restrictions on the available packaging sizes, there are small deviations from the target dimensions. In the following, the consignments are referred to according to the respective packaging type: Kraft paper w/ bubble wrap (KP/BW), Polybag (PB), Kraft paper (KP), Bubble wrap (BW).

3.1. Modeling

3.1.1. Modeling of the Packaging. Packaging models are created using an FE mesh consisting mostly of square shell elements. Irregular elements, such as elongated needle-shaped ones or heavily off-centered intermediate nodes, should be avoided, because they can lead to numerical issues. Furthermore, square elements provide more accurate results compared to triangular elements at the same mesh density. The edge lengths of all elements should be roughly equal and significantly greater than the thickness of the shell [14].

For shell elements in RecurDyn only elastic material types are feasible, which will be used with isotropic behavior. This results in the parameters density, thickness, Young's Modulus, Poisson's Ratio and Damping Ratio. The Damping Ratio, representing the ratio between the stiffness matrix and damping matrix, is utilized to evaluate the damping matrix, as it cannot be directly determined using finite element formulation [24], [25]. The thickness will be measured from the real consignment and the density adjusted accordingly to match the real mass. Poisson's Ratio will be set 0.4 for plastic and 0.1 for kraft paper. The Young's Modulus and Damping Ratio will be investigated in section 3.2, while the following section demonstrates the modeling of the packaging from the four chosen consignments.

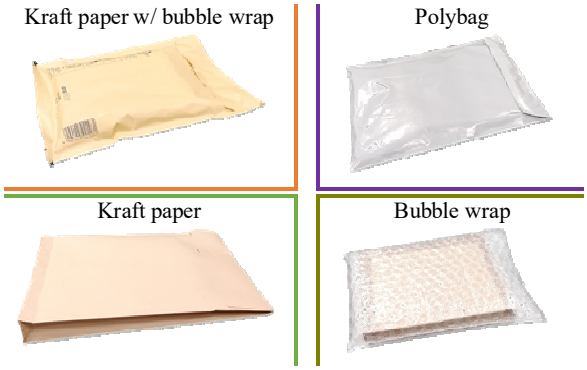

Fig. 11. Overview of real-world consignments used as model templates in this study.

Table 1

Cluster centroids found by Stadlthanner et al. [21]. The grayed-out rows were not considered in the present study

Cluster	Cluster-size	Packaging	Shape	Moveability of the content	multi-part content	Flexibility	Filling level	Length [cm]	Width [cm]	Height [cm]	Mass [g]
1	75	Kraft paper w/ bubble wrap	flat	TRUE	FALSE	1	3	27	19	2	140
2	60	Kraft paper w/ bubble wrap	flat	FALSE	FALSE	1	4	23	16	2	80
3	24	Polybag	flat	FALSE	FALSE	2	4	29	22	2	180
4	17	Kraft paper	flat	FALSE	FALSE	1	4	33	25	3	380
5	16	Kraft paper	flat	TRUE	FALSE	1	3	32	20	2	140
6	11	bubble wrap	flat	FALSE	FALSE	1	4	16	13	2	80

Table 2

The four consignment types investigated in the present study.
KP/BW: Kraft paper w/ bubble wrap; PB: Polybag; KP: Kraft paper; BW: Bubble wrap

Consignment	Based on cluster	Length [cm]	Width [cm]	Height [cm]	Length content [cm]	Width content [cm]	Height content [cm]	Mass [g]
KP/BW	1	27.5	20	2	16.5	12.5	2	140
PB	3	31.5	22.5	2	31	22.5	2	180
KP	4	32	25	3	31	22.5	3	380
BW	6	20	15	2	16.5	12.5	2	80

Kraft paper w/ bubble wrap (KP/BW), Polybag (PB)

The modeling process for the KP/BW and PB packaging is largely the same. A surface is converted into an FE mesh in the mesher and discretized using quadratic shell elements with length of 10 mm. This body represents a packaging half, which is then duplicated. By overlapping and then joining the edge nodes of both bodies, a complete body consisting of two packaging halves is created[1]. The resulting body from this process represents the packaging model of PB (see Fig. 12, indicated by the purple framing), however, to complete the KP/BW packaging an additional step is required.

To model the 1 cm wide glued strip, an extra row of doubled thickness square shell elements is attached to the outside. The expanded process is shown in Fig. 12, indicated by the orange framing.

Kraft paper (KP)

The next packaging is wedge-shaped and consists of multiple layers. Mirroring real-world conditions, the initial folded state is replicated using primarily quadratic shell elements, with triangular elements employed where necessary to reconstruct the eight layers required, as illustrated in Fig. 13. The layers are interconnected by merging them at corresponding edges with their adjacent layers, forming a unified body that represents the packaging.

To unfold the structure, external uniform forces are applied to the nodes of the turquoise layer, as shown in Fig. 14, while the nodes of the brown layer are fixed using boundary conditions.

This process of building the model from the initial folded state enables an accurate depiction of the structural dynamics and behavior of the packaging. It particularly allows the model to "remember" its initial state and the stresses acting on it.

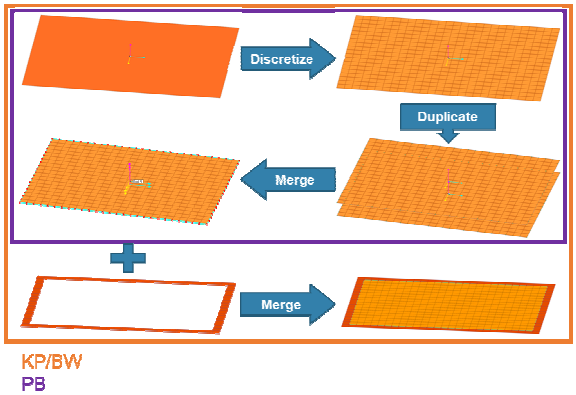

Fig. 12. Modeling the packaging of KP/BW and PB.

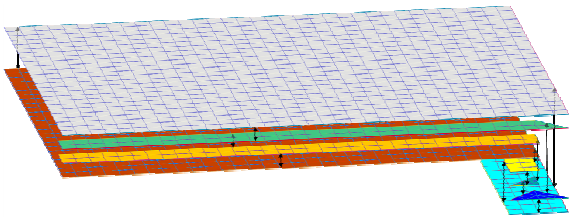

Fig. 13. Layers of the KP packaging.

[1] The corresponding elements share the edge nodes of the target body, while the edge nodes of the source body are deleted.

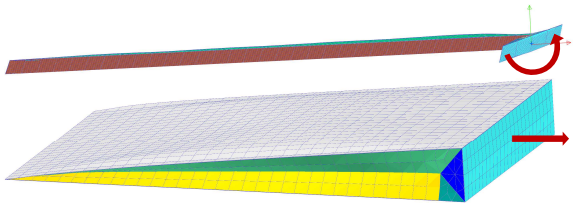

Fig. 14. Steps to unfold KP.

Bubble wrap (BW)

To realistically depict the rounding of the short sides of the BW packaging in comparison to the welded sides, a different approach is employed. Initially, a flat surface is discretized using quadratic 5 mm shell elements. Subsequently, boundary conditions are applied to the edge nodes of the right half to fixate all translational degrees of freedom (DoF), while the other edge nodes are connected via a Force Distributing Rigid (FDR) element, which is similar to RBE2 of other FE software [24]. A torque is then applied at this FDR element to rotate the left half until it overlaps with the fixated nodes, as illustrated in Fig. 15.

Following this, the model is split into two bodies, each of which is duplicated and rotated by 180 °, as illustrated in Fig. 16. The upper bodies are merged with each other, as are the lower bodies, resulting in separate upper and lower body components.

The final step involves merging the remaining two bodies at their edge nodes to complete the resulting packaging model of BW, as shown in Fig. 17.

3.1.2. Modeling of the Contents. The main distinction between the contents of the consignments is whether they are rigid or flexible. Consignments KP/BW, KP and BW contain cuboid cardboard boxes that can be

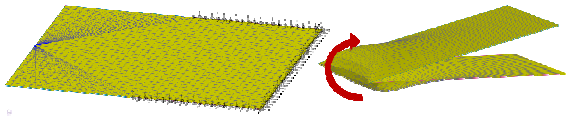

Fig. 15. Modeling of BW packaging using FDR element, boundary conditions (left) and an external torque (right).

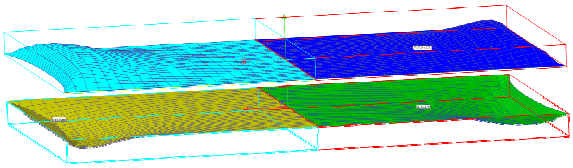

Fig. 16. Merging upper bodies and lower bodies.

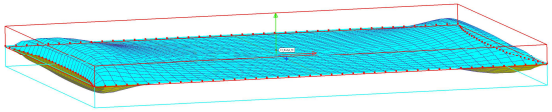

Fig. 17. Resulting packaging model of BW.

efficiently modeled as rigid bodies, since the deformation of the contents is much less than the deformation of the packaging. Therefore, the content modeling process is the same for those consignment types, except for their dimensions and mass.

Rigid Contents (KP/BW, KP and BW)

During transportation, rigid objects like cuboid cardboard boxes maintain their structural integrity and exhibit stiff responses to applied loads. Therefore, modeling them as rigid bodies is effective. A simple cuboid with rounded edges, as shown in Fig. 18, can serve as a representative model. For each content, only density adjustments are needed, along with the geometric parameters.

Flexible Content (PB)

For modeling deformable or flexible contents, finite volume elements are a well-suited approach. Finite volume elements make it possible to simulate the flexibility of materials, whereby the deformations and movements of flexible contents under different loads can be precisely modeled. Fig. 19 displays a finite volume element model obtained by discretizing a cuboid with rounded edges that represents the content of PB. The model mainly uses Solid8[2] elements with an edge length of 10 mm, along with additional elements such as Solid6, Solid5, and Solid4, which have similar edge lengths.

By combining rigid body models for rigid contents and finite element models for flexible contents, it is also possible to realistically model multi-part contents in a wide variety of combinations.

3.1.3. Integration into the Consignment. The process of placing contents into packaging is the same for all consignments, except for KP, which will be discussed later. Before proceeding, it is necessary to implement contacts. Surface contacts will be used for this purpose. These contacts calculate the resulting contact forces, as described in section 2, using the penetration depth between the nodes of the action body (in this case, the nodes of the packaging) and the surface of the base body (which, in this case, is the content). It is important for the normal vectors to be oriented correctly. Specifically, the vectors of the content should point outward and those of the packaging should point inward, as shown in Fig. 20. This means that the upper layer should face downwards and the bottom layer should face upwards.

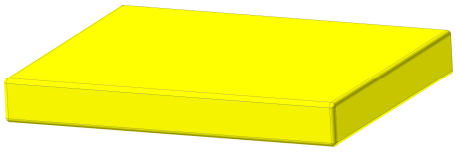

Fig. 18. Model of the content as a rigid body.

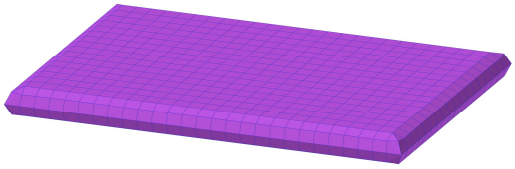

Fig. 19. Model of the content as a flexible body.

[2] Solid8 = 8-node hexahedron; Solid6 = 6-node wedge; Solid5 = 5-node pyramid; Solid4 = 4-node tetrahedron

After implementing contacts, the next step is to apply an external, equally distributed force at the nodes of the top and bottom layers. This force should be reversed in sign and of equal magnitude for the respective layers, as shown in Fig. 21.

The contact between the inside of the packaging and the outside of the contents should only be activated after the opening height is large enough. Otherwise, the penetration depth would be too high, resulting in massive contact forces. This is achieved by deactivation and reactivation of contacts throughout the simulation process. After reaching the desired opening height, the contacts are activated, and the opening force is reduced to zero. This allows the packaging to adapt to the contours of the contents, completing the model. Subsequently, the consignment model can be exported and imported into a new model without losing any information about its initial state[3]. Figure 22 shows the completed models for consignments KP/BW, PB and BW.

To fulfill the condition of limited moveability of its content (see Table 1), an additional step is required for KP. A stiff connection between its packaging and content is necessary, which can be achieved by using an FDR

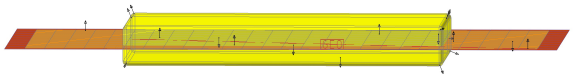

Fig. 20. Contact between packaging and content.

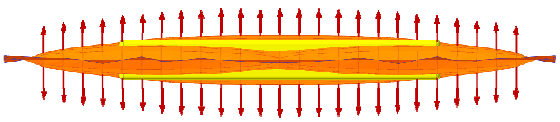

Fig. 21. Forces to separate layers.

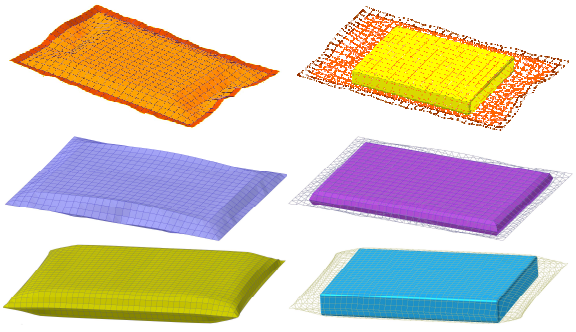

Fig. 22. Complete models for consignments KP/BW, PB and BW.

[3] This is made possible by RecurDyn's "extract" function, which allows to export simulation results into a new model file. In addition to saving position and orientation data, it also preserves prestresses on finite element bodies, which is particularly important to ensure accurate representation.

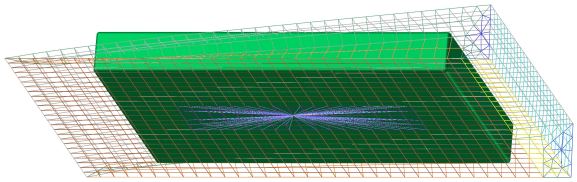

Fig. 23. FDR element connected to the content.

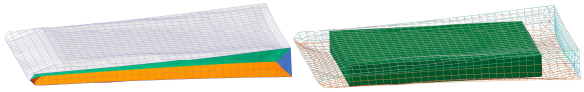

Fig. 24. Complete model for KP.

element at the bottom layer. The nodes are connected in the size of a glue stripe, as shown in Fig. 23.

Once the content is placed on the bottom layer, the FDR element and the content are fixed together to restrict movement. The model is then completed using the same procedure as shown before for the other consignments, which results in the completed consignment model as shown in Fig. 24.

3.2. Parameterization

To ensure accurate representation of real-world conditions in computational simulations, precise parameterization is essential. Design of Experiments (DoE) offers a structured approach to this task. In this study simple yet informative experiments are used that minimize both real-world effort and simulation time to investigate various parameters crucial for our model, as outlined in *Table 3*. The parameterization procedure for KP/BW will subsequently be shown.

Swing test

The swing test involves fixing 2 cm of the consignment's length and allowing the consignment to swing freely from a horizontal position, as shown in Fig. 25. The displacement of the free end in the x-direction[4] is measured to provide information on Young's Modulus and Damping Ratio. Only the maximum displacement for the first and second swing is measured in order to minimize computational resources, and because two swings are deemed sufficient to gather information on the damping behavior.

Table 3

Investigated parameters

Parameter	Unit
Young's Modulus	[MPa]
Damping Ratio	[–]
Stiffness Coefficient Packaging to Content	[N/mm]
Damping Coefficient Packaging to Content	[Ns/mm]
Stiffness Coefficient Packaging to Ground	[N/mm]
Damping Coefficient Packaging to Ground	[Ns/mm]

[4] Horizontal direction of Fig. 25 along the shown ruler.

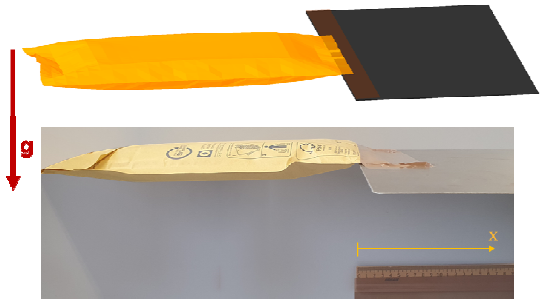

Fig. 25. Comparison of real-world and simulation setup for the swing test.

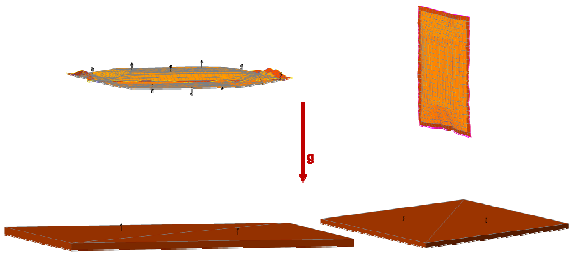

Fig. 26. Setup for the drop tests.

Drop tests

The consignment is released from a horizontal and vertical resting position of 20 cm under gravitational acceleration (see Fig. 26). The purpose of this test is to collect data on the impact behavior of the consignment, including contact parameters and deformation upon impact. Consignments are subjected to impacts at multiple points during handling, which is the primary cause of their deformation and therefore an appropriate test. To conduct this test and for further usage on sorting and conveying systems, the model must be extended by implementing additional contacts. This includes a surface contact between the packaging and the ground, and specifically for vertical impact, a line contact between the edge of the packaging and the ground.

The rebound height serves as benchmark value.

4. RESULTS

4.1. Real-world tests

In this section, as an example, the results of the experiments conducted on KP/BW are presented. The snapshots showcase the values obtained from real-world tests, which serve as the targets for the Simulation Model.

For the first swing, the displacement in the x-direction[4] was recorded at 127 mm, while for the second swing, it measured 32 mm as shown in Fig. 27.

Moving on to the drop tests, the consignment underwent both vertical and horizontal drops onto a metal sheet, simulating real-world impact scenarios. Upon vertical impact, the consignment exhibited a rebound height of 7 mm, whereas a horizontal drop resulted in a rebound height of 4 mm, as shown in Fig. 28.

Fig. 27. Real-world swing test results.

Fig. 28. Real-world drop test results.

Table 4

Factor value ranges for LHS

Parameter	Unit	Value range
Young's Modulus	[MPa]	500 to 5000
Damping Ratio	[–]	10^{-4} to $5 \cdot 10^{-3}$

4.2. Simulation

Swing tests

The swing test employs the parameters young's modulus and damping ratio. Using Latin Hypercube Sampling, an experimental design comprising 100 experiments with factor limits specified in Table 4 is utilized.

A surrogate model is constructed using regression analysis based on the results of the conducted test plan. To achieve this, the Python scikit-learn [19] module is utilized, specifically employing Gaussian Process Regression (GPR). GPR is a non-parametric regression analysis method based on Gaussian processes, which is capable of modeling complex non-linear relationships in data [26].

To determine the most appropriate regression model, the dataset is first divided into two parts. 90% of the data is used for training to identify the best regression model, while the remaining 10% is used for validation purposes. K-fold cross-validation is then employed to select the best regression model.

This method divides the dataset into k randomly selected subsets, or folds, of roughly equal size. During each iteration, the regression model is trained on $k - 1$ subsets while the remaining subset is used as the test dataset. This process is repeated k times, with each subset serving as the test dataset once. The performance indicator for the regression models is the average root mean squared error (RMSE) for the predictions across all k iterations [26].

In this scenario, a 5-fold cross-validation is performed. The GPR model with the Matern covariance function generated the best model predictions. The predictions for the remaining data resulted in an RMSE of 32.17 and 268.74. Residual plots comparing the surrogate model predictions to the remaining test data for validation are shown in Fig. 29.

Contour plots are used to graphically represent the surrogate models, which are generated with the whole dataset. The color and contour lines indicate the resulting values. The value being targeted is denoted by a green line. This results in the diagrams displayed in Fig. 30.

Drop tests

A different approach is taken here, as there are six parameters to test that would require a significantly larger number of simulation runs to thoroughly understand their behavior. Therefore, a screening process is performed prior to the detailed test design.

The purpose of screening is to determine the effects of the parameters on a reference characteristic - in this case, rebound height. The goal is to identify those parameters that have a significant influence on the reference characteristic and therefore are further investigated.

A 2-level full factorial design of 64 trials is used to conduct the screening and is applied to both types of drop tests. The results are illustrated in Fig. 31, which shows the response plots. A multi-factor ANOVA[5] analysis is then performed to identify significant parameter values, with a predefined alpha threshold of 5%. Significant values are highlighted in green, while non-significant values are highlighted in red.

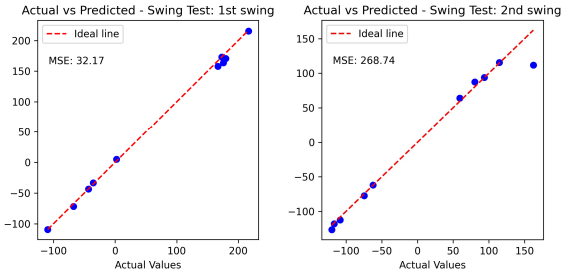

Fig. 29. Residual plots of the swing test.

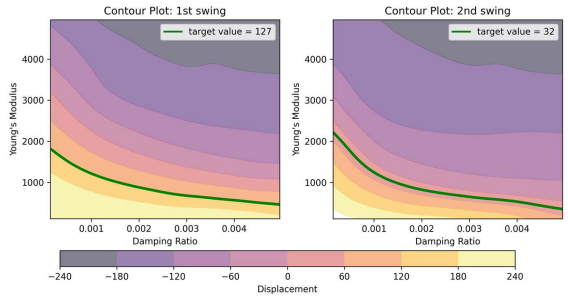

Fig. 30. Contour plots of the surrogate models for the swing test.

[5] In a multi-factor ANOVA, the analysis assesses the impact of multiple factors simultaneously on the variation in the response variable.

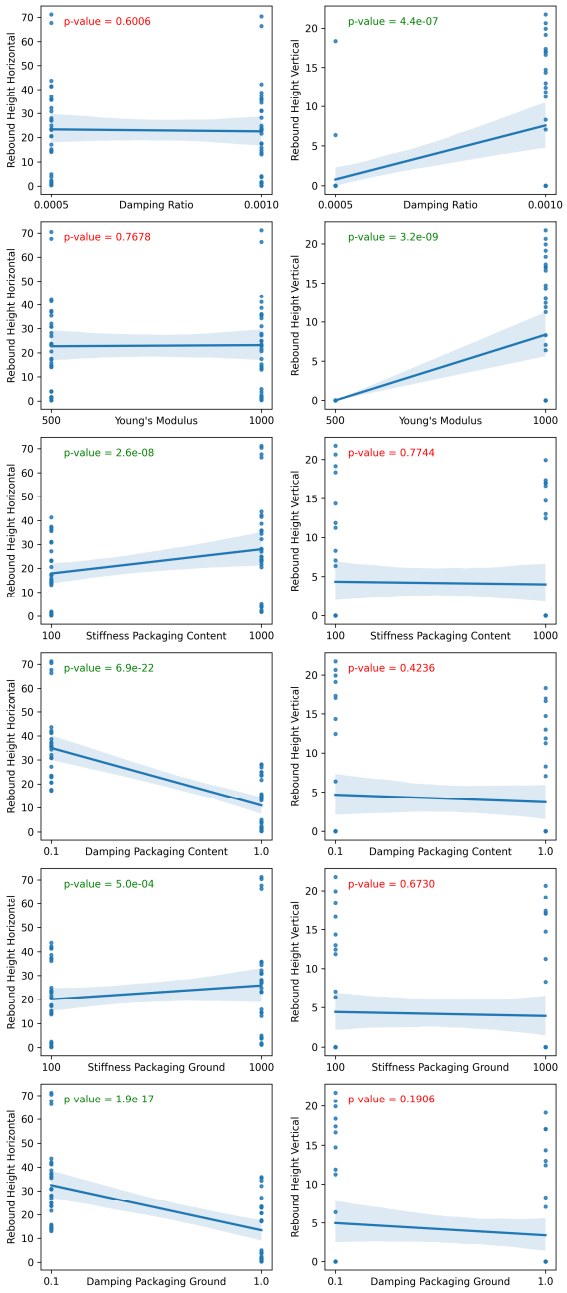

Fig. 31. Response plots of the drop tests (left: vertical, right: horizontal resting position).

For the experiment with a vertical initial position, the contact parameters seem to have a small effect. On the other hand, in the right plots, which include the rebound from a horizontal resting position, it can be seen that the Damping Ratio and Young's Modulus have little effect on the experiment. Therefore, these parameters will not be varied in the respective experiments.

After screening, the effects of significant parameters are thoroughly investigated using Latin Hypercube Sampling. An experimental design comprising 500 experiments for the vertical drop test and 100 experiments for the vertical one is used, with parameter limits shown in Table 5.

Table 5

Factor value ranges for LHS

Parameter	Unit	Value range
Young's Modulus	[MPa]	200 to 2000
Damping Ratio	[–]	10^{-4} to $5{\cdot}10^{-3}$
Stiffness Coefficient Packaging to Content	[N/mm]	100 to 1000
Damping Coefficient Packaging to Content	[Ns/mm]	0.1 to 1
Stiffness Coefficient Packaging to Ground	[N/mm]	100 to 1000
Damping Coefficient Packaging to Ground	[Ns/mm]	0.1 to 1

To create surrogate models for the drop tests, the same process as in the swing test is used, resulting in GPR models with the Matern covariance function. The predictions for the remaining data resulted in a RMSE of 4.11 and 2.19 for the drop test from a vertical and horizontal position, respectively. Fig. 32 shows residual plots comparing the surrogate model predictions to the remaining test data for validation.

Contour plots are employed to visually represent the surrogate models, generated using the entire dataset. These plots use color and contour lines to indicate the resulting values, with the targeted value denoted by a green line. Fig. 33 displays the contour plot for the vertical drop test.

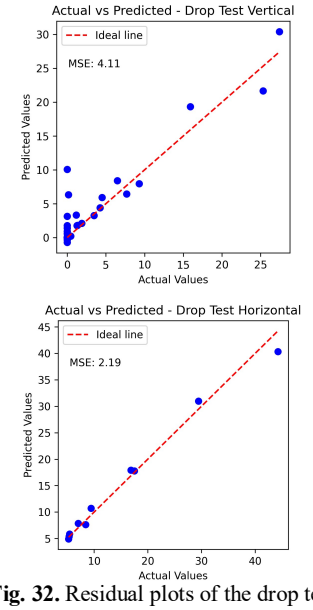

Fig. 32. Residual plots of the drop tests.

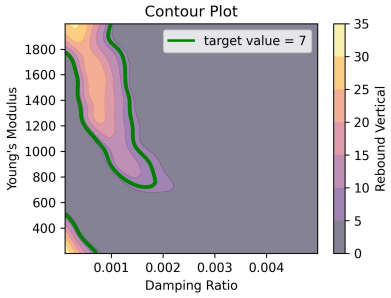

Fig. 33. Contour plot drop test vertical.

Fig. 34. Comparison of two distinct behaviors in the simulation upon impact to the real-world test.

In examining the contour plot of the vertical drop test, it is evident that most parameter combinations result in a rebound of less than 5 mm. Two distinct areas show significantly higher rebound. Upon closer inspection, these areas exhibit contrasting behaviors.

In the lower-left region, characterized by low values of Young's Modulus and Damping Ratio, the packaging demonstrates high flexibility. As a result of impact, the content makes direct contact with the floor and causes the packaging to buckle (see Fig. 34, left).

In contrast, the second area, marked by higher Young's Modulus values, portrays a stiffer packaging. Here, the 1 cm thick edge acts like a spring upon impact, resulting in a pronounced rebound (see Fig. 34, right). The latter behavior largely corresponds to observations in practice (see Fig. 34, middle).

In essence, the differences in rebound underscore the importance of Young's Modulus in determining the impact response.

For the horizontal drop test, no contour plots are generated. This is due to the high dimensionality caused by the number of factors involved, which makes it impractical to represent the relationships between the factors and the response in a meaningful way.

4.3. Parameter Optimization

After constructing surrogate models through Latin Hypercube Sampling (LHS) and regression analysis, the parameter optimization proceeds using Eq. (11), where the weights are determined by the inverse of the range between the highest and lowest response values observed in the LHS plans. The resulting parameter are shown in Table 6.

Using these parameter values, the experiments were repeated to validate the results. The results are shown in Table 7.

For the swing test, the simulation duration is 1.4 seconds, with a computational time[6] of 384 seconds. The observed response value for the first swing is 128 mm and 27 mm for the second swing.

In the vertical drop test, the simulation duration is 0.3 seconds, with a computational time of 125 seconds and a rebound height of 6.2 mm. Similarly, for the horizontal drop test, the simulation duration is also 0.3 seconds, with a computational time of 76 seconds and a rebound height of 4.5 mm.

[6] All simulations were carried out on a test system featuring an Intel i9-13900H processor utilizing 4 cores.

Table 6

Resulting parameter values from the optimization

Parameter	Unit	Values
Young's Modulus	[MPa]	926
Damping Ratio	[–]	$1.71 \cdot 10^{-3}$
Stiffness Coefficient Packaging to Content	[N/mm]	649
Damping Coefficient Packaging to Content	[Ns/mm]	0.579
Stiffness Coefficient Packaging to Ground	[N/mm]	611
Damping Coefficient Packaging to Ground	[Ns/mm]	0.591

Table 7

Simulations with the parameter settings

Experiment	Simulation Duration [s]	Computational Time [s][6]	Response Values [mm]	Target Values [mm]
Swing test: 1st swing	1.4	384	128	127
Swing test: 2nd swing			27	32
Drop test vertical	0.3	125	6.2	7
Drop test horizontal	0.3	76	4.5	4

4.4. Application of the modeled consignments to a sorting process

In order to evaluate the feasibility of these models for practical use, a simulation setup with a conveying process was created. The goal is to investigate whether it is possible to simulate not only individual consignment, but also the bulk behavior of multiple consignment. For this purpose, all four modeled consignments are placed on a conveyor belt with deflectors.

Shell elements are used to model the conveyor belts. The movement of the belt, which has a velocity of 1.6 meters per second, is realized by driven rollers, where one roller is rotatably mounted and the other is rotated by a motion specification. To complete the model, two rigid bodies fixed in space were implemented as deflectors. The deflectors are set at an angle of 45 ° and extend almost to the center of the conveyor belt.

The static and dynamic coefficients of friction for the contacts between the consignments to the belts and the deflectors, which are seen as metal sheets, are taken from a study by Schadler et al. [8], where they tested cardboard, kraft paper and polybags on an X6Cr17 steel plate and a polyurethane belt.

Figure 35 illustrates the results of the study, showing the initial placement of the consignments, their disposition after one second, and the final image at the two-second mark as the consignments exit the conveyor. The results show a high level of detail in describing the interactions between the consignments. However, a limitation became apparent: the considerable

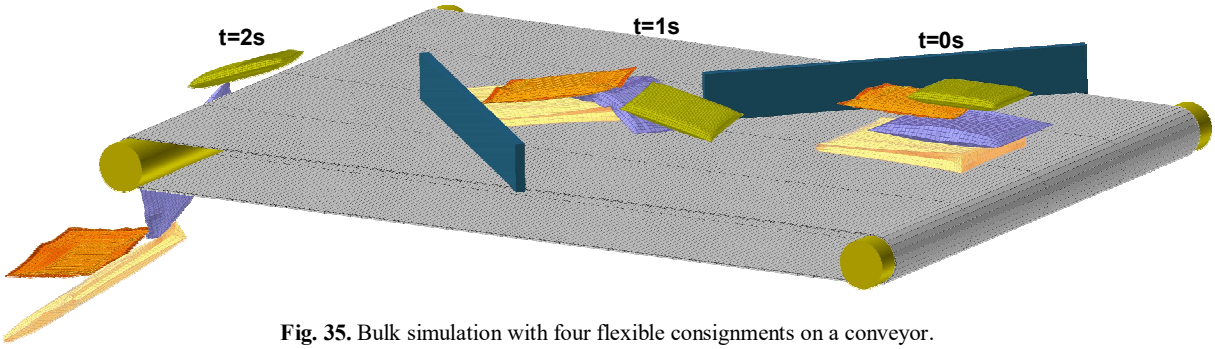

Fig. 35. Bulk simulation with four flexible consignments on a conveyor.

computational time required, which amounted to 24 hours for two seconds of simulated time on the same test system as used for the parameterization simulation runs.

5. CONCLUSION AND FURTHER RESEARCH

In this work, a structured approach for the development of a simulation model for the modeling of the motion behavior of flexible consignments was pursued. A methodology has been presented that starts with the characterization of the properties, followed by the description of the modeling possibilities and their concrete application to real consignments and their parameterization.

The paper deals with step 3 and step 4 of this methodology, while step 1 and step 2 have been covered in previous research studies. Step 3 of this methodology deals with the systematic bottom-up modeling of four consignments, beginning with the packaging and the contents, by using multi flexible body dynamics.

The packaging model was built from shell elements and the contents were added, depending on their flexibility, as rigid bodies or volume elements, to create the consignment models. Step 4 of this methodology deals with parameterization and was demonstrated using one consignment as an example. Swing and drop tests were chosen as experiments. The real-world tests were employed to determine target values, while the corresponding simulations were used to investigate the effects of the model parameters through the use of DoE and to generate surrogate models. These surrogate models were then used for parameter optimization with the objective of minimizing the discrepancy between the prediction of the surrogate model and the target values derived from the real tests. This process ultimately enabled the determination of the optimal parameter values. Finally, to assess the viability of these models for practical use, the bulk behavior of multiple consignments on a conveyor belt with deflectors was simulated.

While this approach excels at representing individual or small groups of consignments in detail in a reasonable computational time, an alternative strategy is essential for efficiently simulating a large number of flexible consignments in a shorter time frame. Short computation times are essential when training surrogate models that require large amounts of data, generated by large simulation studies, to accurately predict the material flow of bulk consignments. To reduce the computational effort required, a shift to less detailed representations of the behavior of individual consignments is necessary, while prioritizing the efficient representation of the global behavior of the bulk.

Future research by the Institute of Logistics Engineering (Graz University of Technology) will address this problem through a multi-fidelity approach that incorporates computational models of different levels of detail. The goal is to exploit the complementary strengths of these models to improve the predictive capabilities of surrogate models. In this context, MFBD can serve as the high-fidelity model, while other less accurate but faster approaches can be utilized as the low-fidelity model. Identifying and developing an appropriate low-fidelity model represents the subsequent step in the process of achieving the goal of a multi-fidelity model.

In summary, this work represents a significant advancement in the field of simulating the movement behavior of flexible consignments in the sorting process, thereby contributing to the development of innovative sorting and conveying technologies.

Funding:

This paper was written as part of the project "ISAAK - Entwicklung eines Simulationsansatzes zur Analyse von Kleinsendungen" funded by the Austrian Research Promotion Agency (FFG) within the BRIDGE program.

Author Contributions:

Conceptualization: G.L., D.S., A.O-P. C.L.; Methodology: G.L., D.S., A.O-P.; Software: G.L.; Validation: G.L.; Formal analysis: G.L.; Investigation: G.L., D.S.; Resources: C.L.; Writing - Original Draft: G.L., D.S.; Writing - Review & Editing: G.L., D.S., A.O-P., C.L.; Visualization: G.L.; Supervision: C.L.; Project administration: G.L., D.S., C.L.; Funding acquisition: C.L.

REFERENCES

[1] KE-CONSULT Kurte&Esser GbR, *KEP-Studie 2023 – Analyse des Marktes in Deutschland* (CEP Study 2023 - Analysis of the market in Germany), Bundesverband Paket und Expresslogistik e. V. (BIEK), 2023.

[2] M. Schadler, D. Stadlthanner, B. Mayer, M. Schedler, C. Landschützer, *A method for pre-sorting mixed mail*

using convolutional neural networks and transfer learning, in *MHCL 2022: XXIV International Conference*, Belgrade: Faculty of Mechanical Engineering, Belgrade University, 2022, S. 71–80.

[3] M. Fritz, A. Wolfschluckner, D. Jodin, *Simulation von Paketen im Pulk* (Simulation of parcels in bulk), *Vol. 2013*, S. Issue 11, 2013.

[4] M. Fritz, *Beitrag zur Simulation des Bewegungsverhaltens von Stückgütern im Pulk im Kontext der Vereinzelung* (Contribution to the simulation of the movement behavior of general cargo in bulk in the context of separation), Graz University of Technology, 2016.

[5] M. Fritz, D. Jodin, *Untersuchung der Dynamik von Stückgütern auf Stetigförderern – Analyse, Simulation und Laborversuche* (Investigation of the dynamics of general cargo on continuous conveyors - analysis, simulation and laboratory tests), *Vol. 2016*, S. Issue 10, 2016, doi: 10.2195/LJ_PROC_FRITZ_DE_201610_01.

[6] D. Kaever, *Systematische Betrachtung von Technologien für den Umschlag von Paketen im Pulk und deren Simulation mit der Diskrete-Elemente-Methode* (Systematic consideration of technologies for the handling of parcels in bulk and their simulation with the discrete element method), 2021. doi: 10.25673/60071.

[7] C. Landschützer, *Methoden und Beispiele für das Engineering in der Technischen Logistik* (Methods and examples for engineering in technical logistics). in publication series of the Institute of Logistics Engineering. Verlag der Technischen Universität Graz, 2018.

[8] M. Schadler, M. Schedler, M. Knödl, D. Prims, C. Landschützer, A. Katterfeld, Characteristics of ‚polybags' used for low-value consignments in the mail, courier, express and parcel industry, *Vol. 2022*, S. Issue 01, 2022.

[9] S. Roth, *Simulation von flexiblen Polybags und Untersuchung deren Umlenkverhaltens mittels Mehrkörper-Simulations- Modellen* (Simulation of flexible polybags and investigation of their deflection behavior using multi-body simulation models), master thesis, 2019.

[10] G. Rill, T. Schaeffer, F. Borchsenius, *Grundlagen und computergerechte Methodik der Mehrkörpersimulation: Vertieft in Matlab-Beispielen, Übungen und Anwendungen* (Fundamentals and computer-oriented methodology of multi-body simulation), Wiesbaden: Springer Fachmedien Wiesbaden, 2020,

[11] M. Schedler, C. Landschützer, *Methodische Entwicklung eines neuartigen Sortiersystems für Polybags* (Methodical development of a new sorting system for polybags), *Vol. 2021*, S. Issue 17, 2021, doi: 10.2195/LJ_PROC_SCHEDLER_DE_202112_01.

[12] G. Leitner, D. Stadlthanner, and A. Ortner-Pichler, *Modellierung von forminstabilen Kleinsendungen mittels Multi Flexible Body Dynamics* (Modeling of dimensionally unstable small consignments using Multi Flexible Body Dynamics), in press, 2024.

[13] J. Choi, J. H. Choi, *Analysis Method for Multi-Flexible-Body Dynamics Solver in RecurDyn*, *Trans. KSME C Ind. Technol. Innov.*, Bd. 3, Nr. 2, S. 107–115, Juni 2015, doi: 10.3795/KSME-C.2015.3.2.107.

[14] S. Vajna, C. Weber, K. Zeman, P. Hehenberger, D. Gerhard, S. Wartzack, *CAx für Ingenieure: Eine praxisbezogene Einführung* (CAx for engineers: A practical introduction). Berlin, Heidelberg: Springer, 2018. doi: 10.1007/978-3-662-54624-6.

[15] A. A. Shabana, O. A. Bauchau, G. M. Hulbert, *Integration of Large Deformation Finite Element and Multibody System Algorithms*, *J. Comput. Nonlinear Dyn.*, Bd. 2, Nr. 4, S. 351–359, Okt. 2007, doi: 10.1115/1.2756075.

[16] J. Choi, H. Ryu, J. Choi, *Multi flexible body dynamics using incremental finite element formulation*, ECCOMAS Thematic Conference, Warsaw, Poland, 29 June-2 July, 2009.

[17] J. Choi, *A Study on the Analysis of Rigid and Flexible Body Dynamics with Contact,* Seoul National University, 2009.

[18] J. Choi, H. S. Ryu, C. W. Kim, J. H. Choi, *An efficient and robust contact algorithm for a compliant contact force model between bodies of complex geometry*, *Multibody Syst. Dyn.*, Bd. 23, Nr. 1, S. 99–120, Jan. 2010, doi: 10.1007/s11044-009-9173-3.

[19] F. Pedregosa *et al.*, *Scikit-learn: Machine Learning in Python*, *J. Mach. Learn. Res.*, Bd. 12, Nr. 85, S. 2825–2830, 2011.

[20] J. A. Nelder, R. Mead, *A Simplex Method for Function Minimization*, *Comput. J.*, Bd. 7, Nr. 4, S. 308–313, Jan. 1965, doi: 10.1093/comjnl/7.4.308.

[21] D. Stadlthanner, H. Steinkellner, C. Landschützer, D. Kaever, *Hierarchical Density-Based Clustering of Mixed-Mail in Austria*, submitted 2023.

[22] J. C. Gower, *A General Coefficient of Similarity and Some of Its Properties*, *Biometrics*, Bd. 27, Nr. 4, S. 857, Dez. 1971, doi: 10.2307/2528823.

[23] L. McInnes, J. Healy, S. Astels, *hdbscan: Hierarchical density based clustering*, *J. Open Source Softw.*, Bd. 2, Nr. 11, S. 205, März 2017, doi: 10.21105/joss.00205.

[24] FunctionBay, Inc., *V9R5 RecurDynManual*. 2021. [Online]. Verfügbar unter: https://functionbay.com/en

[25] B. Klein, *FEM: Grundlagen und Anwendungen der Finite-Element-Methode im Maschinen- und Fahrzeugbau* (FEM: Fundamentals and applications of the finite element method in mechanical and vehicle engineering), 10, verb. Aufl. in Lehrbuch. Wiesbaden: Springer Vieweg, 2015. doi: 10.1007/978-3-658-06054-1.

[26] K. Siebertz, D. van Bebber, T. Hochkirchen, *Statistische Versuchsplanung: Design of Experiments (DoE)*, 2. Auflage. in VDI-Buch. Berlin [Heidelberg]: Springer Vieweg, 2017. doi: 10.1007/978-3-662-55743-3.